NJC

Accepted Manuscript

This is an *Accepted Manuscript*, which has been through the Royal Society of Chemistry peer review process and has been accepted for publication.

Accepted Manuscripts are published online shortly after acceptance, before technical editing, formatting and proof reading. Using this free service, authors can make their results available to the community, in citable form, before we publish the edited article. We will replace this *Accepted Manuscript* with the edited and formatted *Advance Article* as soon as it is available.

You can find more information about *Accepted Manuscripts* in the Information for Authors.

Please note that technical editing may introduce minor changes to the text and/or graphics, which may alter content. The journal's standard Terms & Conditions and the Ethical guidelines still apply. In no event shall the Royal Society of Chemistry be held responsible for any errors or omissions in this *Accepted Manuscript* or any consequences arising from the use of any information it contains.

ROYAL SOCIETY OF CHEMISTRY

www.rsc.org/njc

Arsenate removal from contaminated water by highly adsorptive nanocomposite ultrafiltration membrane

Rasoul Jamshidi Gohari[a,b], Woei Jye Lau[a], Elnaz Halakoo[a], Ahmad Fauzi Ismail[a*], Fatemeh Korminouri[a], Takeshi Matsuura[a,c], Mohammad Saleh Jamshidi Gohari[b], Md. Najmul Kabir Chowdhury[a]

[a] Advanced Membrane Technology Research Centre (AMTEC), Universiti Teknologi Malaysia, 81310 Skudai, Johor, Malaysia
[b] Department of Chemical Engineering, Islamic Azad University, Bardsir Branch, Bardsir, Iran
[c] Department of Chemical and Biological Engineering, University of Ottawa,161 Louis Pasteur St., Ottawa, ONK1N6N5, Canada

Abstract

In order to overcome the limitations of adsorption process, a new type of nanocomposite ultrafiltration (UF) membrane consisted of polyethersulfone (PES) and titanate nanotubes (TNTs) was fabricated in this work via the phase inversion technique and used for adsorptive arsenate (As(V)) removal. The effects of impregnating TNTs on the structural morphology, hydrophilicity, porosity, pure water permeability and As(V) uptake capacity of the nanocomposite membranes were studied for different weight ratio of TNT:PES in the membrane matrix, ranging from 0 to 1.5. Of the membranes studied, As(V) uptake capacity as high as 125 mg/g was able to achieve using the membrane containing the highest amount of TNTs (designated as PES/TNT-1.5) and the performance of this membrane is comparable to most of the available adsorbents and other As removal systems. Increasing TNT:PES weight ratio from 0 to 1.5 led to the increase of membrane pure water permeability from 39.4 to 1250 L/m^2.hr.bar with water contact angle decreased from 69.5^o to 5.2^o. The experimental findings from the continuous UF process revealed that the nanocomposite membrane of the highest TNTs content could generate high permeate quality to meet the maximum As level set by the World Health Organization (WHO), i.e. <10 µg/L. Furthermore, the adsorptive performance of nanocomposite membrane could be easily regenerated using alkaline solution.

Keywords: *As(V) removal, nanocomposite, titanate nanotubes, ultrafiltration, adsorptive membrane*

*Corresponding author: afauzi@utm.my; fauzi.ismail@gmail.com

1. Introduction

Arsenic (As) contaminated drinking water is a major public health worldwide problem. The existence of As in drinking water has been reported in more than 70 countries.[1] It has been previously evaluated that millions of people, mainly in developing countries such as India and Bangladesh were at high risk as a result of drinking As-contaminated waters.[2] In natural environment As can occur in several oxidation states (−3, 0, +3, +5), but in aqueous medium it is predominantly found in inorganic form as oxyanions of arsenite (As(III)) and arsenate (As(V)), which may exist in ground and surface water, respectively.[1,3] In aqueous solution, As is not easily detected by sight as it is colorless and odorless.[4] Because of this, its contamination is a serious concern for the environment and living creatures.

Previous study has shown that long-term exposure to drinking water contaminated with As can inevitably lead to various kinds of cancers such as bladder, lungs, skin and kidney.[3] Therefore, in order to minimize these health risks, in January 2001, US Environmental Protection Agency (EPA) has set the As standard for drinking water, aiming to reduce As concentration to 10 μg/L by 2006.[5] Conventional As removal technologies such as chemical precipitation, coagulation and flocculation and ion exchange and membrane filtration could be used to remove As.[6-13] However, to efficiently decrease As concentration to acceptable levels as required by the law, all the above mentioned technologies experience or be subjected to one or more drawbacks, restrictions and practicability. For example, extra post-treatment process is needed to remove adsorbents from water source after adsorption process, which indirectly increases the overall cost of treatment. Membrane filtration processes such as nanofiltration (NF) and reverse osmosis (RO) on the other hand can be operative method for As elimination. But, they require high-energy consumption as a result of high pumping pressure. Low-pressure driven membrane processes like microfiltration (MF) and ultrafiltration (UF) are porous enough to pass molecules of true solution and cannot remove the dissolved As species from As-contaminated water.[14] The inconsistent and/or incomplete removal of As using conventional technologies has prompted the quest for efficient, environmental friendly and low cost treatment technology for hazardous As decontamination.

It is undeniable that the adsorption technique is presently one of the most effective and economical options for As removal; particularly for natural water with low concentrations of the element.[3, 7,15] Nano-scale metal oxides have attracted a lot of research interest as promising arsenic adsorbent because of their high adsorption capacity and selectivity.[16-18] Nano-sized ferric oxides,[19] manganese oxides (MnO),[20] titanium dioxide[21] and Fe–Mn binary oxide[22] are some of the adsorbents that have been evaluated for their efficiencies in removing As from aqueous solution. However, the use of nano-scale metal oxides alone in fixed-bed columns or any other flow-through system for heavy metal decontamination is not very practical due to excessive pressure drops and also separation of nanoparticles after treatment from the water sources is quite challenging.[17]

To further promote the practical usage of nano-scale metal oxide adsorbents in real water and wastewater treatment, many researchers have attempted to impregnate metal oxide nanomaterials into porous host materials namely carbon,[15] bentonite,[23] zeolite,[24,25] diatomite,[25,26] cellulose[12,27,28] and porous membrane.[29-32] Among the host media studied, membranes made of polymeric materials have distinctive advantages owing to their tunable surface pore size, chemistry as well as mechanical properties.[17]

Previously, our research team successfully synthesized a new type of adsorptive microporous UF membranes that were composed of organic polyethersulfone (PES) and inorganic Fe–Mn binary oxide nanomaterial for As(III) removal.[32] In order to further improve the adsorptive rate of membrane against As, we will explore a new type of nanomaterial, titanate nanotubes (TNTs), in this work. This nanomaterial could be prepared via hydrothermal process and has been previously reported to exhibit outstanding sorption to arsenic.[33]

TNTs have been successfully investigated to remove toxic heavy metals due to their high surface area, large amount of functional hydroxyl (-OH) groups on the surface and low point of zero charge (pHpzc). Almost all protons of the -OH functional groups can be simply exchanged with transition heavy metal ions such as Pb^{2+}, Cd^{2+}, Cu^{2+} and Cr^{3+}.[33-35] In addition to these heavy metals, Niu *et al.*[33] reported that TNTs could achieve adsorption capacity as high as 208 and 60 mg/g for As(V) and As(III), respectively.

To the best of our knowledge, there is no research work reporting the use of TNTs for adsorptive membrane preparation for As removal process. Thus, the main focus of the present study is centered on producing high performance PES/TNTs

adsorptive microporous membranes for effective decontamination of As(V) from aqueous solutions. To achieve this objective, PES/TNTs adsorptive membranes with various weight ratios of TNTs to PES, which ranged from 0 to 1.5, were cast while the other casting parameters were maintained constant. Prior to the evaluation of membrane adsorption capacity against As(V), the membrane properties with respect to morphology, surface hydrophilicity, pure water permeability and overall porosity were first characterized. The experiments on batch adsorption, continuous filtration as well as regeneration of the adsorption capacity of membrane were also performed in this study.

2. Experimental

This section covers the types of materials used to fabricate the asymmetric flat sheet PES/TNT nanocomposite membranes based on the dry-wet phase inversion process by casting the dope solutions consisted of different weight ratio of TNT:PES as well as the experimental procedure and methods used to evaluate the performance of the nanocomposite membranes for removing As(V) in batch and continuous experiments. At last, evaluation on the regeneration capability of nanocomposite membranes was also performed.

2.1 Chemicals

All chemicals used in this work were of analytical grade. Polyethersulfone (PES, Radel® A300, Mw = 58,000 g/mol) in pellet form was purchased from Amoco Chemicals. N-methylpyrrolidinone (NMP) and polyvinylpyrrolidone (PVP, Mw = 25,000 g/mol) as solvent and additive, respectivley, sodium hydroxide (NaOH) and hydrochloric acid (HCl, 37%) were all supplied by Merck. Titanium dioxide (TiO_2) Degussa P25 nanoparticles supplied by Evonik Industries were used as received to synthesize TNTs. Sodium arsenate dibasic heptahydrate ($NaHAsO_4 \cdot 7H_2O$) from Sigma Aldrich was employed to prepare As(V) stock solution by dissolving it in DI water.

2.2 Synthesis of TNTs

TNTs were synthesized through hydrothermal method as described by Niu *et al.*[33] Firstly, 3 g of TiO_2 nanoparticles (P25, Degussa) was added into 100 mL of 10 M NaOH aqueous solution. After vigorous stirring for 12h, the milk-like mixture was

moved into a 150 mL Teflon-lined autoclave container and heated at 180^{o}C in an electric oven for 10 h. After the completion of hydrothermal process, the temperature of the Teflon-lined autoclave was decreased to ambient temperature naturally. The white product was then taken out from autoclave container and rinsed several times with DI water. Then, the samples were washed with 0.5 M HCl solution until pH became 7-8. Finally, protonated TNTs were dried overnight at 100^{o}C, followed by grinding into fine powders.

2.3 Fabrication PES/TNTs membranes

In this study, phase inversion method was used to produce flat sheet PES (control) and PES/TNTs adsorptive membranes. Initially, pre-weighed amount of pore forming agent (PVP) was dissolved in NMP, followed by adding a precise amount of TNT into the mixture and stirring under continuous stirring. Then, the suspension was sonicated for 12 h to prevent TNTs agglomeration before the addition of PES. Pre-determined amount of dried PES pellets was gradually added to the solution that was under continuous stirring at temperature of 60^{o}C. The resulting homogeneous dope solutions were again sonicated for 30 min to remove air bubbles. Table 1 presents the compositions and viscosity of all six casting solutions. Attempt was also made to prepare membrane using dope solution containing TNT/PES ratio of >1.5, but this membrane was unable to form due to the excessive use of inorganic nanofillers in polymeric matrix. The viscosity of the dope solution was determined using a digital viscometer (Cole-Parmer). To fabricate a flat sheet membrane, the homogeneous dope solution was cast onto a smooth and clean, flat glass plate using a self-made casting knife, following 30 s solvent evaporation in air of ~70% relative humidity. The glass plate together with the cast film was then immersed into a DI water bath to induce phase inversion. After the membrane was peeled off from the glass plate, it was transferred to another DI water bath and stored for 3-4 days at room temperature to remove any residual solvent.

Table 1: Composition and viscosity of PES/TNTs dope solution.

Membrane	TNT/PES ratio	PES (wt%)	PVP (wt%)	NMP (wt%)	TNT (wt%)	Viscosity (cp)
PES	0	15.00	1.50	83.50	–	203
PES/TNT-0.125	0.125	14.72	1.47	81.96	1.84	235
PES/TNT-0.25	0.25	14.45	1.44	80.48	3.61	265
PES/TNT-0.5	0.5	13.95	1.40	77.67	6.98	357
PES/TNT-1.0	1.0	13.04	1.30	72.60	13.04	570
PES/TNT-1.5	1.5	12.24	1.22	68.18	18.36	986

2.4 Batch adsorption experiments

Adsorption behavior of As(V) by PES/TNT adsorptive membranes was investigated using batch procedure. As(V) solutions with initial concentrations ranging from 10 to 200 mg/L (equivalent to parts per million, ppm) were prepared by dissolving $NaHAsO_4.7H_2O$ into DI water. The solutions were then stored in a refrigerator at 10^oC till use. Batch experiments were performed in Erlenmeyer flasks (250 mL) with 100 mL of As(V) solutions and 0.1 g of adsorptive membrane (which was cut in small pieces), and pH was kept constant at 3 ($\pm$ 0.5) using HCl or NaOH solution. The glass vessels were shaken on a platform shaker at 200 rpm for 24 h at 25 ±1 °C. The concentrations of residual As(V) in the prepared solutions in mg/L level were determined using flame atomic absorption spectrometer (FAAS, pinAAcle900T, Perkin–Elmer). The FAAS instrument was calibrated with As standard solution and the minimum detection limit of it for As(V) was 1 mg/L. All samples were measured twice and the average was recorded. The equilibrium adsorption capacity, q_e (mg/g) of all membranes was calculated by Equation 1.[36,38]

$$qe = \frac{(C_i - C_e)V}{M_m} \quad (1)$$

where C_i (mg/g) and C_e (mg/g) are the initial and equilibrium As(V) solution concentrations, respectively, V (L) is the volume of As(V) solution and M_m (g) is the mass of the dry membrane added in the solution.

The effect of pH on As(V) adsorption was conducted by adding 0.1 g of the membrane with the maximum adsorption capacity to 100 mL of the 40 mg/L As(V) solution at different pH ranging between 2 and 11. After 24 h shaking of the sample at 25 ^{o}C, the concentration of As(V) of each pH solution was determined by FAAS. After evaluating the membrane's adsorption capacities and determining the optimum pH, batch kinetic experiments were conducted by shaking a series of 250 mL Erlenmeyer flasks containing 0.1 g of the membrane with the highest adsorption capacity and a 100 mL aqueous solution of 30 mg/L of As(V) in optimal pH for different time intervals. The platform shaker speed was set at 200 rpm. On the other hand, the concentration of Ti(IV) ions in the solution due to the possible leakage of TNTs from nanocomposite membrane structure was measured in μg/L level (equivalent to parts per billion, ppb) by an inductively coupled plasma emission spectrometer (ICP-OES; Perkin Elmer Optima 3000 DV). Calibration the ICP-OES analysis was performed with reference solutions containing 5, 10, 20, 40 and 60 μg Ti /L, prepared with a stock solution of 1 mg Ti/L (Merck) and the minimum detection limit was found to be 1 μg/L.

2.5 Continuous UF filtration study

The pure water permeability (PWP) of all produced membranes was obtained employing a homemade cross-flow permeation cell as illustrated in Fig. 1. Prior to the PWP measurement, membrane samples with an effective surface area of 12.56 cm^2 were compacted by filtering DI water at pressure of 3 bars for 1h. PWP of the membranes was acquired at 1 bar using the following equation.

$$J_w = \frac{Q}{A\,\Delta t \Delta p} \qquad (2)$$

where J_w is pure water permeability (L/m^2.h), Q is the quantity of permeate (L), A is the effective membrane area (m^2), Δt is the sampling time (h) and Δp is the trans membrane pressure difference.[39]

The PWP experiment was followed by continuous membrane adsorption tests using PES/TNT-1.5 due to the highest As(V) adsorption capacity of this membrane. Feed tank was loaded with the solution with initial concentration of As(V) (97.5) which is much higher than the safety level recommended by WHO and US EPA for As concentration in drinking water, i.e. 10 μg/L. Filtration tests were carried out at room temperature and 0.1 bar. The cross flow rate was kept constant at 60 L/h. During the

cross flow filtration experiment, a sample of permeate was taken every 30 min and analyzed using Perkin-Elmer atomic absorption spectrophotometer equipped with graphite tube atomizer (GF-AAS). As(V) standard solution (Perkin-Elmer, USA) was diluted to 2, 5, 10, 20 and 40 μg/L to prepare As(V) calibration curve for GF-AAS. The minimum detection limit of the As concentration that gives an answer equivalent to three times the standard deviation of blank was 1 μg/L. When the As(V) concentration in the permeate surpassed 10 μg/L, the back-washing was carried out using the 0.1 M NaOH solution to regenerate membrane before subjecting the same membrane to subsequent As(V) removal experiments.

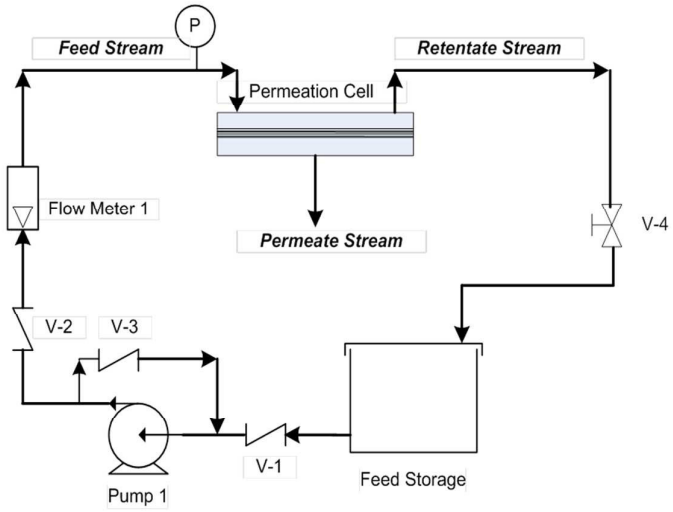

Fig.1. Schematic apparatus of cross-flow membrane filtration system.

2.6 Characterizations

The morphology and dimension of the synthesized TNT sample synthesized in this work were characterized using transmission electron microscope (TEM) (HT 7700, Hitachi). Prior to TEM analysis, the fine TNTs were ultrasonically dispersed in absolute alcohol for 10 min. X-ray diffraction (XRD) scans of the synthesized TNTs, PES membrane and PES/TNTs adsorptive membrane were determined at room temperature using an X-ray diffractometer (D5000, Siemens). Fourier transform infrared (FTIR) spectra of the synthetic TNTs before and after As(V) adsorption were obtained at ambient temperature on a Thermo Nicolet 5700 infrared spectrometer. The measured wave number range was between 4000 and 500 cm^{-1}. The membrane's

surface hydrophilicity was characterized using a contact angle goniometer (OCA15pro, Dataphysics Instrument GmbH Filderstadt) based on the sessile drop technique. DI water was applied as the probe liquid. In order to mitigate the experimental error, the recorded contact angles were average values from at least 10 different arbitrary locations on the dry membrane surface. For surface roughness and pore size determination, membrane samples in a scan size of 5 μm ×5 μm, were imaged using atomic force microscope (AFM) (Seiko SPA-300HV, Japan) and the membrane's pore sizes were determined using the visual inspection of line profiles of various pores from the AFM images which were taken from different areas of the same membrane as described by Singh *et al.*[40]

In order to examine the top surface and cross section of the PES and PES/TNTs membrane, scanning electron microscope (SEM) combined with energy dispersive X-ray (EDX) were used (TM3000, Hitachi). Before scanning, all samples were coated with a thin layer of gold to provide electrical conductivity. The membrane's cross-sections were prepared by snap-freezing the flat sheets in liquid nitrogen. The overall porosity *(ε)* of the membranes was acquired gravimetrically and calculated using Equation 3:[36]

$$\varepsilon = \frac{W_w - W_d}{\rho_{water} \times A \times l} \times 100 \qquad (3)$$

where the weights of the wet and dry membranes (g) represent with W_w and W_d, respectively, A is the flat sheet effective area (cm^2), l is the thickness of wet membrane (cm) and ρ_{water} is the water density at room temperature.

3. Results and discussion

This section discusses the data obtained from different methods on the properties of nanomaterial (TNT) synthesized as well as its effect on the characteristics of PES-based microporous membranes with respect to surface hydrophilicity, roughness, morphology and adsorption capacity against As(V).

3.1 Characterization of the TNTs and membranes

In this section, TNTs properties were first characterized using TEM, XRD and FTIR before they were embedded into polymeric membrane structure to synthesize adsorptive membranes. Several key properties of membrane that are important in water

filtration process are later provided. These include pure water flux; water contact angle, top surface roughness, cross-sectional morphologies and overall structural porosity.

Fig. 2 demonstrates the TEM images of the synthetic TNTs. The uniform and tubular structure of TNTs with the length of 250–300 nm and outer diameter of 9–10 nm can be seen in the figure.

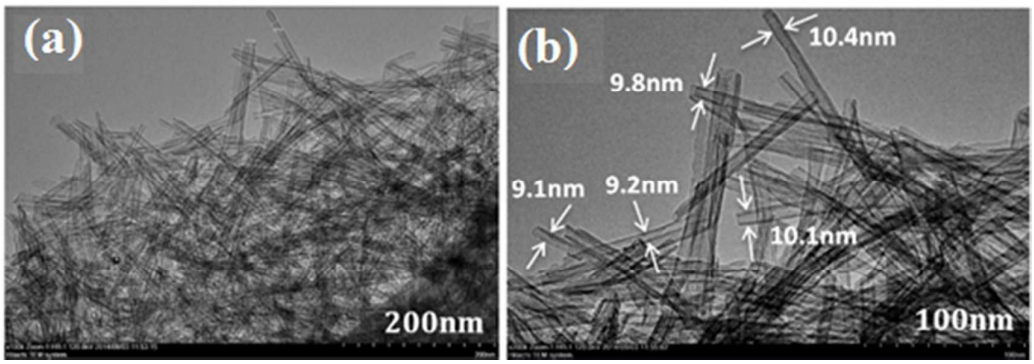

Fig.2: TEM images of the presence of TNTs at two different scale bars, (a) 200 nm and (b) 100 nm.

The existence of TNTs in the structure of the membrane was further analyzed by XRD and the results are shown in Fig. 3. The 2θ peaks at 10.9°, 24.7° and 48.5° are the typical characteristic peaks of TNTs that can be obviously seen in the XRD pattern of Fig. 3(a). As a comparison, the PES membrane (Fig. 3(b)) displayed one broad XRD peak at 2θ of 18.04° which can be attributed to its amorphous structure. The presence of obvious peak at 11.5° in the PES/TNT membrane indicated the effective integration of TNTs in the PES matrix (Fig. 3(c)).

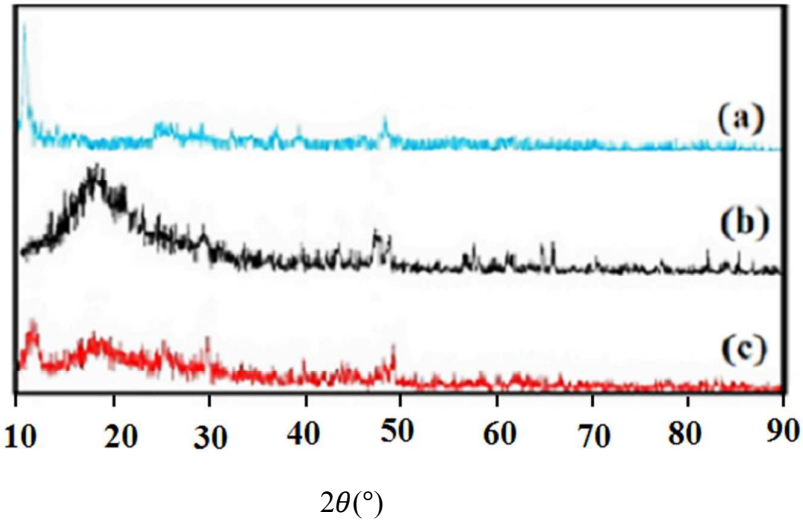

Fig.3. XRD scans of (a) TNT, (b) PES and (c) PES/TNT-1.0.

Fig. 4 shows the FT-IR spectra of TNTs before and after As(V) adsorption. Fig. 4(a) presents a series of absorption bands for the pure TNTs at 3241, 1606 and 933 cm^{-1}. Multi-layered TNTs were reported to compose of Na_xH_{2-x} Ti_3O_7 (x∽0.75) in which 1606 cm^{-1} band is correlated to the H-O–H bending vibration coupled with Ti atoms while strong absorption peak at 3241 cm^{-1} is specified to the O–H stretching vibration, owing to the existence a large amount of water and hydroxyl groups in TNTs.[37] The band at region of 933 cm^{-1} might be attributed to stretching vibration of a four-coordinated Ti-O.[37,41] As shown in Fig. 4(b), after As(V) was being adsorbed by TNTs, a slightly change was detected at the band of 929 cm^{-1}, suggesting no positive effect of Ti-O and TiO_6 on As(V) adsorption. It can also be observed that the band of the Ti–OH groups in unabsorbed TNTs was considerably shifted to the right from 3241 to 3361cm^{-1} in As(V)-adsorbed TNTs. This revealed that As(V) uptake by TNTs arise via electrostatic interactions between As(V) and the Ti–OH functional group after replacement of hydrogen ions.

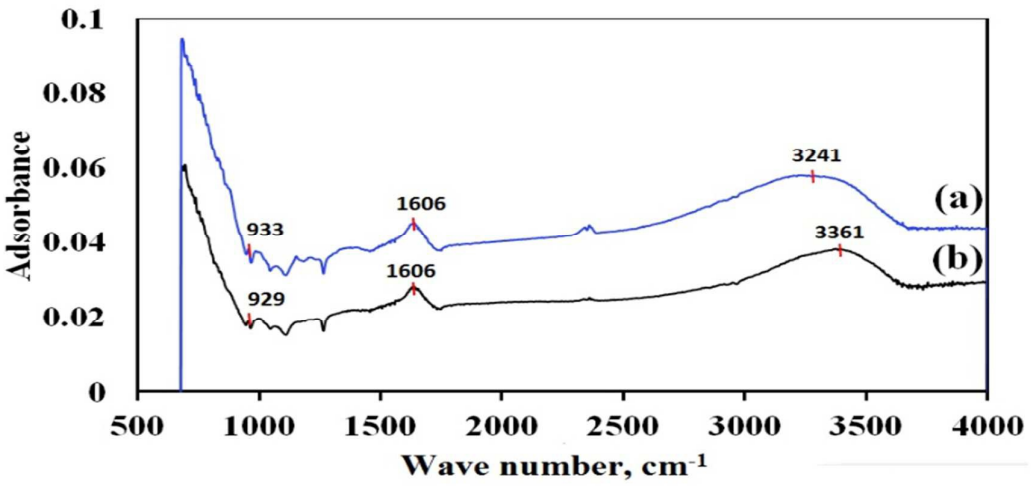

Fig. 4: FTIR spectrum of TNT particles before (a) and after (b) arsenate adsorption experiments.

Fig. 5 shows the shape of water droplet on the surface of membrane made of different content of TNTs. Surface hydrophilicity is one of the prominent membrane properties. A membrane with excellent surface hydrophilicity in general demonstrates promising feature in improving membrane water permeability. As can be seen, the significant decrease of membrane contact angle from 69.5º for the PES membrane to around 5.2º for the PES/TNT-1.5 membrane suggested the remarkable improvement in membrane hydrophilicity. The improved membrane hydrophilicity resulted from embedding TNTs in PES matrix is most likely due to the existence of large amount of hydroxyl groups in TNTs as evidenced from FTIR result.

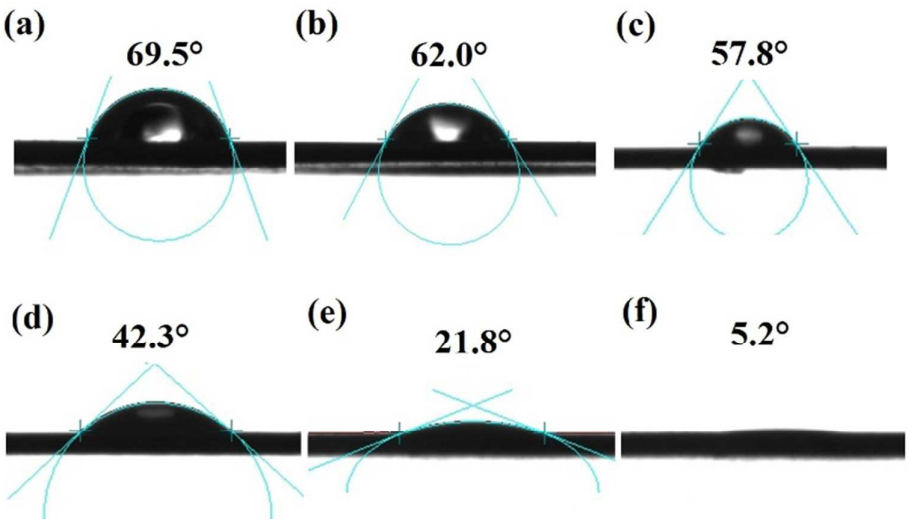

Fig.5. Shape of a small water droplet (0.5 μL) on the top surface of (a) PES, (b) PES/TNT-0.125, (c) PES/TNT-0.25, (d) PES/TNT-0.5, (e) PES/TNT-1.0 and (f) PES/TNT-1.5 membrane.

Fig.6 shows the atomic-level resolution 3D AFM top surface images of all the membrane samples prepared in this work. The presence of TNTs in PES membrane matrix has a prominent influence on the surface of the membrane and subsequently membrane pore size and porosity (see Table 2). R_a value, as indicated in Fig. 6, increased significantly from 2.92 nm in neat PES membrane to >43 nm in TNT/PES-1.5 with the increase of TNT/PES weight ratio from 0 to 1.5. This can be attributed to the alignment of TNTs embedded in membranes.

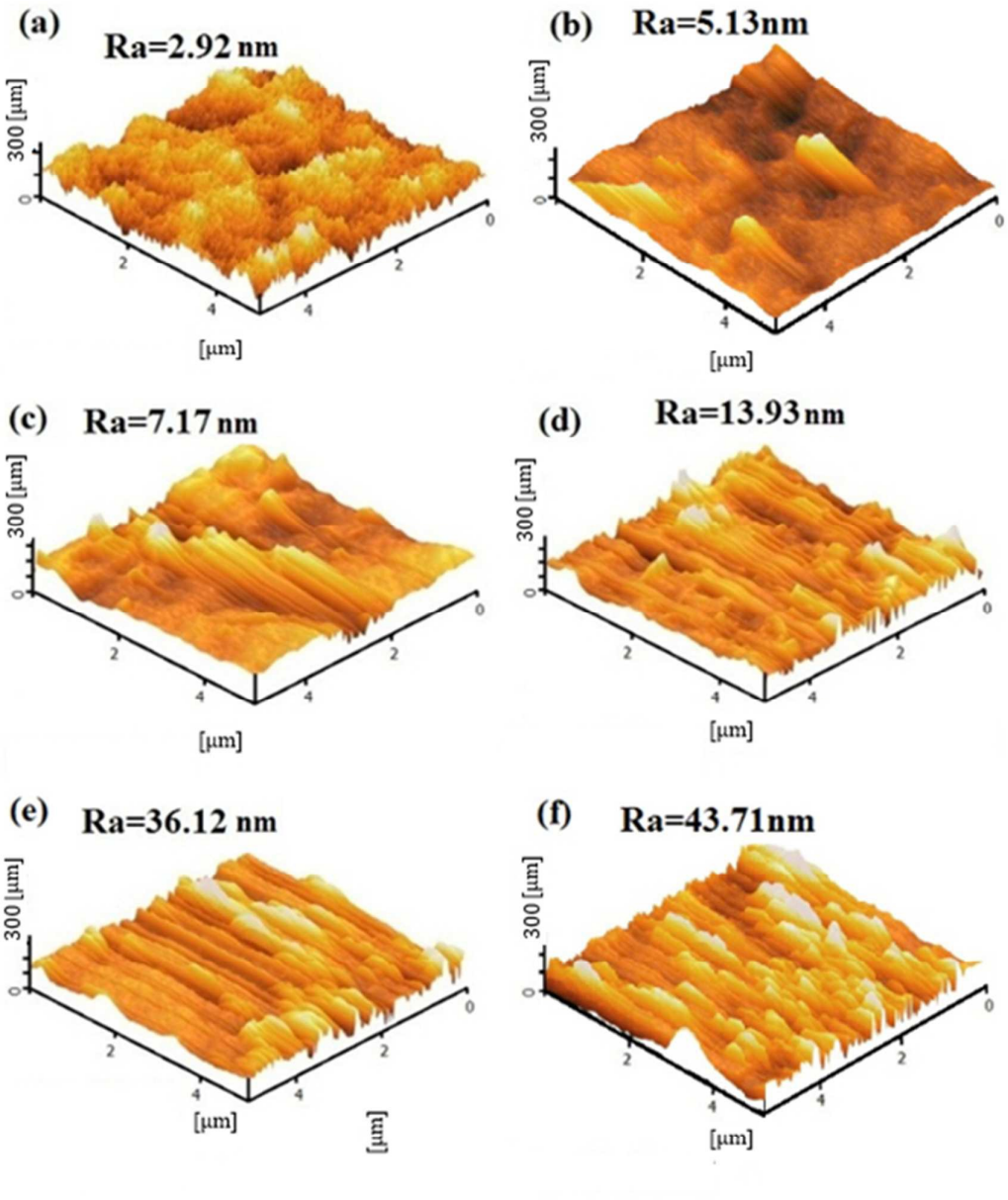

Fig.6: 3D AFM top surface images of the plain and modified membranes with different TNTs/PES ratios, (a) PES, (b) PES/TNT-0.125, (c) PES/TNT-0.25,(d) PES/TNT-0.5, (e) PES/TNT-1.0 and (f) PES/TNT-1.5.

Fig. 7 represents the top surface, bottom surface and cross-sectional SEM micrographs of all prepared membranes with different TNT/PES weight ratio. The SEM images showed the presence of tube-like structures (i.e. TNTs) on the top and bottom surface of all membranes embedded with TNTs without any significant

nanotube mass agglomeration. The results suggest the well-distributed TNTs in the polymer matrix. Furthermore, from the EDX analysis (see Fig. 8) on the top and the bottom surfaces of the all-adsorptive membranes prepared, the detection of nearly similar Ti atomic element confirmed the uniform dispersion and existence of TNTs in the membrane matrix.

The SEM cross-sectional images, on the other hand, revealed that all fabricated membranes have the typical asymmetric structure with more fine finger-like structure beneath a top skin layer. The vertical fine finger-like structure near the top skin layer was enlarged with increase in the weight ratio of TNT:PES from zero to 1.5. Additional information on the surface morphology of the prepared membranes in terms of pore size and porosity were also investigated and are provided in Table 2 together with the permeate flux of the membranes. It was found that porosity enhanced while pore size decreased as TNT/PES weight ratio increased during membranes preparation.

Table 2: Pure water permeability, overall porosity and pore size of all fabricated membranes.

Membrane	Pure water permeability ($L/m^2.h.bar$)	Overall porosity (%)	Pore size (nm)
PES	39.4	80.50	146.6
PES/TNT-0.125	232.0	81.15	122.5
PES/TNT-0.25	622.1	82.00	106.2
PES/TNT-0.5	716.6	86.13	85.7
PES/TNT-1.0	970.5	88.40	72.4
PES/TNT-1.5	1250.0	90.10	68.5

In general, the high porosity (80.5-90.1%) value obtained from all membranes prepared could be attributed to low polymer concentration used in the casting solution and the addition of pore forming agent, i.e. PVP. The addition of TNTs has further improved membrane porosity as TNTs with super-hydrophilic in nature could play a prominent role in enhancing the solvent and non-solvent exchange rate during the phase-inversion process, leading to higher membrane porosity.[42]

On the other hand, the surface pore size was gradually decreased from 146.6 nm for PES membrane to 68.5 nm for PES/TNT-1.5 membrane. The decrease in the

pore size may be explained by the increase in the viscosity of the casting solution upon addition of TNTs (viscosity data in Table 1) that might have suppressed the formation of membrane pore. From these results, it can be inferred that the addition of TNTs in casting solution is capable of enhancing overall surface porosity and promoting formation of finger-like structure as well. However, it should be noted that the enhanced membrane performance is attributed to the enhancement of membrane surface hydrophilicity with TNTs integration due to abundance of hydrophilic hydroxyl groups on the membranes surface. The enhanced membrane hydrophilicity resulted from TNTs addition is consistent with the FTIR patterns observed and contact angle results.

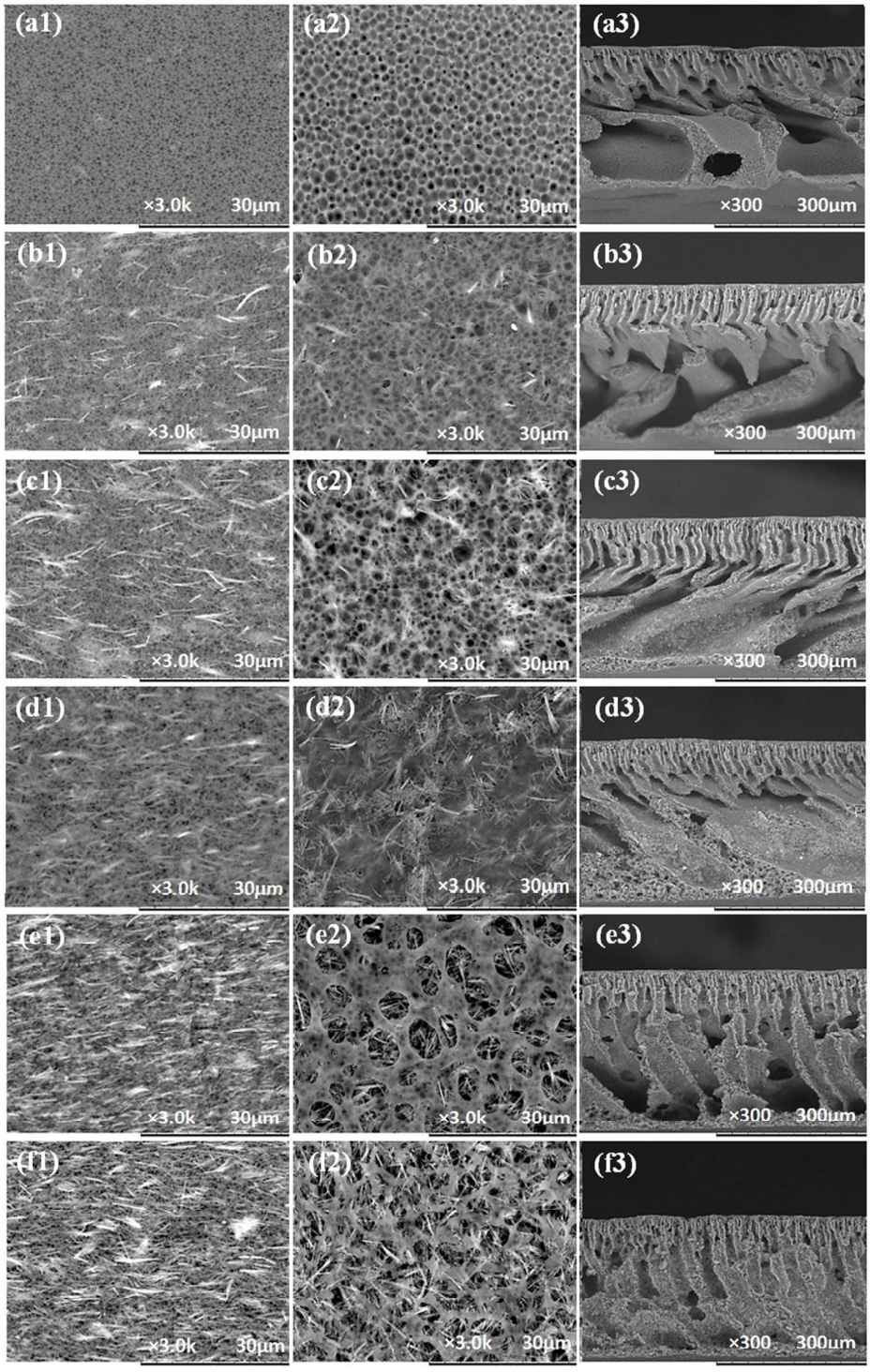

Fig. 7: SEM micrographs of top surface (1), bottom surface (2) and cross section (3) of membranes prepared with different TNT:PES weight ratios, (a) PES,(b) PES/TNT-0.125, (c) PES/TNT-0.25,(d) PES/TNT-0.5, (e) PES/TNT-1.0 and (f) PES/TNT-1.5.

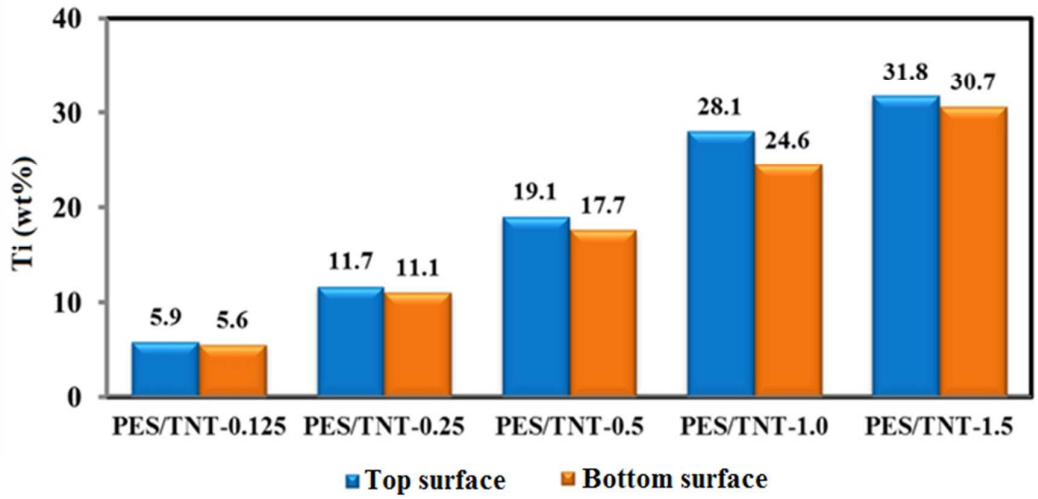

Fig. 8: EDX analysis on the membranes surface (top and bottom) with respect to Ti element.

3.2 Arsenic Adsorption studies

In this section, the effect of pH on membrane adsorption capability against As(V) together with its isotherm and adsorption kinetics will be performed in order to provide insights into the performance and mechanisms of adsorptive membrane embedded with TNTs for As(V) removal.

3.2.1 pH effect study

The pH is considered as one of the most imperative features governing removal of As(V) from aqueous solutions and the most prominent parameter controlling the absorption of heavy metal ions on adsorbents. This can be partly ascribed to strong competitive nature of hydrogen ions with heavy metal ions to position adsorption sites .[43] The removal efficiency of As(V) as a function of pH is shown in Fig. 9 along with the detection of titanium ions leakage (from nanocomposite membrane) during adsorption process. In this experiment, PES/TNT-1.5 membrane was used since it achieved the highest adsorption capacity among all the membranes studied. As can be seen, As(V) adsorption occurred more in acidic solution. The As(V) removal was optimum over the pH range of 2.5–3.5 for PES/TNT-1.5 membrane. The predominance of As(V) occurred in forms of $H_2AsO_4^-$ and $H_2AsO_4^{2-}$ over the range of 2.5–11.5 pH.[44] At low pH values (2.5–3.5), the surface of impregnated TNTs in

polymeric matrix undergoes protonation reaction (i.e. $\equiv TiOH + H^+ \leftrightarrow \equiv TiOH_2^+$), and increase in the concentration of protonated sites ($\equiv TiOH_2^+$) is supposed to increase the positively charged sites. Consequently, the adsorption the As(V) increases in the lower pH region through surface complexation between arsenic anions and TNTs.[45,46] However, in the higher pH region, the deprotonated sites ($\equiv TiO^-$) dominate, the repulsion effect increases, leading to sharp reduction of arsenate adsorption at pH 7.5–10.7 region. It is also evident from Fig. 9 that the solution contained no titanium ions after absorption process at any initial pH values, which confirms that no leaching of Ti ions arises in the course of adsorption experiment. The results may also depict no existence of Ti ions in the water.

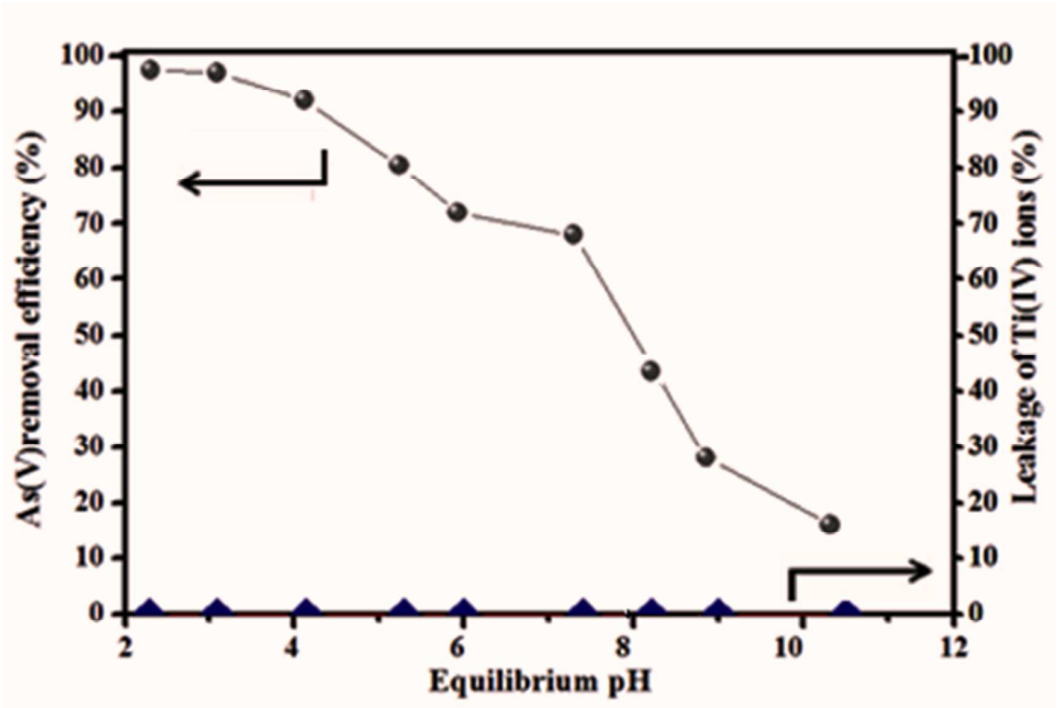

Fig. 9: Effect of initial pH on As(V) removal by PES/TNT-1.5 (Operating conditions: initial concentration of As(V)= 40 mg/L, membrane dose = 1.0 g/L, stirring speed = 200 rpm, temperature = 25^{o}C and contact time = 24 h).

3.2.2 Isotherm analysis

The isotherm experiments information is explained in Fig. 10 for the PES membrane with and without TNT adsorbent particles. It should be pointed out that the experiment results showed the pristine PES membrane have no capacity of adsorbing As(V) due to the absence of TNTs in membrane matrix. While, results show that

increasing TNTs/PES ratio from 0.125 to 1.5 led to remarkable increase of the membrane adsorption capacity. The maximum adsorption capacity of As(V) was achieved at 21.7, 40.2, 66.7, 100.2 and 124.9 mg/g by PES/TNT-0.125, PES/TNT-0.25, PES/TNT-0.5, PES/TNT-1.0 and PES/TNT-1.5 membrane, respectively. The improved adsorption capacity of modified membranes could be associated to the increasing levels of adsorbent available to adsorb As(V).

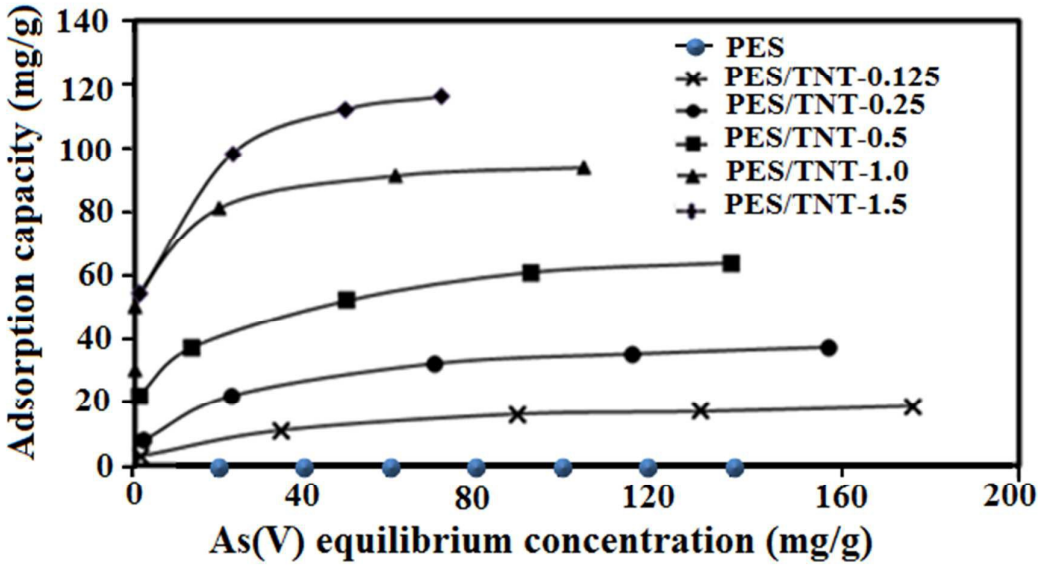

Fig. 10: Adsorption isotherm of As(V) using modified membranes with different TNTs:PES ratio. (Operating conditions: Temperature: 25°C; membrane dose: 1.0 g/Land equilibrium time: 24 h).

Table 3: Comparison of maximum As(V) adsorption capacity for different adsorbents.

As(V) adsorbent	pH	Maximum As(V) adsorption capacity (mg/g)	Ref.
TNT (1.0 g/L)	3.0	208	33
PES/TNTs membrane (1.0 g/L)	3.5	125	This study
Zirconium-immobilized nano-scale carbon	3-4	110	13
Iron oxide coated sponge	6.5-7.3	4.6	47
PVDF/zirconium membrane	3-4	21.5	48
Iron-impregnated tablet ceramic	6.9	4.89	49
Cerium-loaded cation exchange resin	6.0	1.03	50
Iron hydro(oxide) nanoparticles onto activated carbon	7.0	4.65	51
Nanosized iron oxide-coated perlite	6.5-7	0.39	52

Table 4 represents the Langmuir and Freundlich isotherm factors for As(V) uptake on adsorptive membrane at pH 3.5. In order to correlate the equilibrium data, the two most prevalent isotherm models, namely Langmuir and Freundlich model were used as stated in Eqs. (4) and (5), respectively.[32]

$$q_e = \frac{q_{max} b C_e}{1 + b C_e} \quad (4)$$

where q_e is the amount of As(V) adsorbed into the PES/TNT membrane (mg/g) , C_e is the equilibrium As(V) concentration in the solution (mg/L), q_{max} is the highest adsorption capacity of PES/TNT membrane (mg/g) and b is the Langmuir reaction constant (L/mg) related to free energy of adsorption.

$$q_e = K_f C_e^{1/n} \quad (5)$$

where q_e and C_e were previously stated in the Equation (4), K_f(mg/g) is the Ferundlich constant indicator of the adsorption capacity of adsorbent and 1/n is the heterogeneity parameter, corresponding the adsorption intensity. Based on the data obtained, it is shown that the Langmuir model is more appropriate to represent the adsorption isotherm of As(V) for membranes, mainly owning to the greater R^2 value achieved.

Table 4: Langumir and Freundlich isotherm parameters for As(V) adsorption on nanocomposite membranes.

Nanocomposite Membrane	Langmuir model			Freundlich model		
	q_m (mg/g)	b(L/mg)	R^2	K_f(mg/g)	1/n	R^2
PES/TNT-0.125	21.73	0.032	0.998	1.83	0.467	0.966
PES/TNT-0.25	40.10	0.030	0.997	6.59	0.358	0.984
PES/TNT-0.5	66.67	0.128	0.996	16.60	0.284	0.984
PES/TNT-1.0	100.2	0.294	0.999	33.72	0.241	0.831
PES/TNT-1.5	124.9	0.362	0.999	50.11	0.222	0.977

3.2.3. Analysis of adsorption kinetics

Fig. 11 presents the influence of time on kinetics of As(V) adsorption using the membrane with high adsorption capacity, i.e. PES/TNT-1.5 membrane. As it is evident from the figure, there is an increasing trend in the adsorption capacity of PES/TNT-1.5 with increasing the contact time from 0 to 12 h. However, the uptake of As(V) leveled off after 10 h. The mechanism of As(V) adsorption kinetic was determined via analyzing the experimental data using Lagergren's pseudo-first order and pseudo-second order kinetic models based on the Eqs. (6) and (7), respectively.[36]

$$\frac{dq_t}{dt} = K_1(q_{e1}\text{-}q_t) \quad (6)$$

$$\frac{dq_t}{dt} = K_2(q_{e2} - q_t)^2 \quad (7)$$

where q_e (mgg^{-1}) and q_t (mgg^{-1}) are the amount of As(V) adsorbed per gram of membrane, at equilibrium and at time t(h), respectively, k_1(h^{-1}) and k_2 ($mg^{-1}gh^{-1}$) are the rate constants of the pseudo-first order and pseudo-second order kinetic models, respectively. The resultant kinetic factor values from the models are represented in Table 5. The considerable difference in the values of experimental and calculated adsorption capacity calculated was figured out for the first-order kinetics. Whereas, the quantity of adsorption capacity acquired from the second-order kinetics was much the same with the resultant adsorption capability with a large correlation coefficient. Consequently, it can be concluded that Lagergren's pseudo-second order kinetics model can be employed to express the As(V) adsorption kinetics of PES/TNT-1.5 membrane.

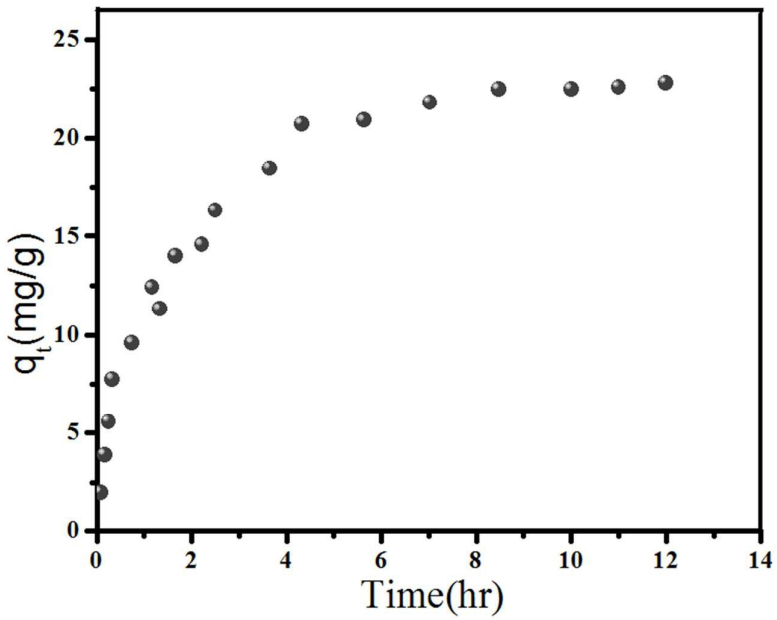

Fig. 11: Variation of As(V) adsorption kinetics onto PES/TNT-1.5 membrane with time. (Operating condition: initial As(V) concentration (C_0)=30 mg/L, Temperature = 25°C; membrane dose= 1.0 g/L and equilibrium time= 12 h).

Table 5: Adsorption kinetic constants obtained by different models.

C_0	$q_{e,exp}$	First-order kinetics model			Second-order kinetics model		
(mg/L)	(mg/g)	q_{e1}(mg/g)	k_1(1/h)	R^2	q_{e2}(mg/g)	k_2(g/mg h)	R^2
30	22.8	16.147	0.0019	0.971	24.57	0.0006	0.996

3.3 Continuous filtration experiment

Using a cross-flow UF filtration system, the continuous performance of the optimum membrane (PES/TNT-1.5) with an effective area of 12.56 cm^2 for As(V) elimination before and after membrane regeneration process is presented in Fig.12. Based on the test results, the unspoiled PES/TNT-1.5, operated at 0.1 bar, demonstrated the ability to maintain the As(V) concentration below the MCL of 10 µg/L for approximately 3850 cm^3 of permeate, before failing to produce high permeate of high quality (with As(V) content < 10 µg/L).

In order to determine the regeneration feasibility of PES/TNT-1.5 membrane adsorbent, desorption experiment was then carried out using strong NaOH solution (0.1 M) to desorb As(V) on PES/TNT-1.5 membrane. Detailed adsorption behavior and mechanism of As(V) removal by TNTs could be found in the work of Niu *et al.*[33] in which the authors analyzed the oxidation state of As species adsorbed on the surface of TNTs using XPS. The results showed that after reaction with As (V), the Ti atom content decreased by 9.5% whereas the content of oxygen atom increased, indicating the introduction of As oxyanions or water molecules. Niu *et al.*[33] also showed the desorption mechanism of As ions at high pH was attributed to competition between OH^- and adsorbed arsenate ions at TNTs embedded in the membrane. To study the regeneration capability of membrane, UF experiment was repeated using the same arsenic solution for feed after the membrane was subjected to regeneration process with 0.1 M NaOH solution. It was found that the permeate As(V) concentration was kept below 10 µg/L until 3620 cm^3 of permeate was collected, with desorption efficiency of 94 % ((1-3620/3850)×100). Thus, the high regeneration feasibility of PES/TNT-1.5 membrane was proven. However, to further promote the practical application of nanocomposite membranes for the long-term performance arsenic decontamination in real water and wastewater treatment, there still exist some critical

technical drawback to be solved. For example, after regeneration process when As is recovered in the concentrated form; the highly controversial issue is how to dispose the concentrated As solutions. One outstanding method to treat concentrated As is encapsulation via solidification/stabilization followed by disposal of treated wastes in secure landfills.[44] It has been previously demonstrated that As concentrates could be incorporated into Portland cement or Portland cement and iron (II). However, this technique has not been effectively proceeded.[44,53,54] General speaking, heavy metals decontamination by nanocomposite membrane is still in the infant stage and further experimental research is required to inaugurate a commercial technique for using it on a wide-range application.

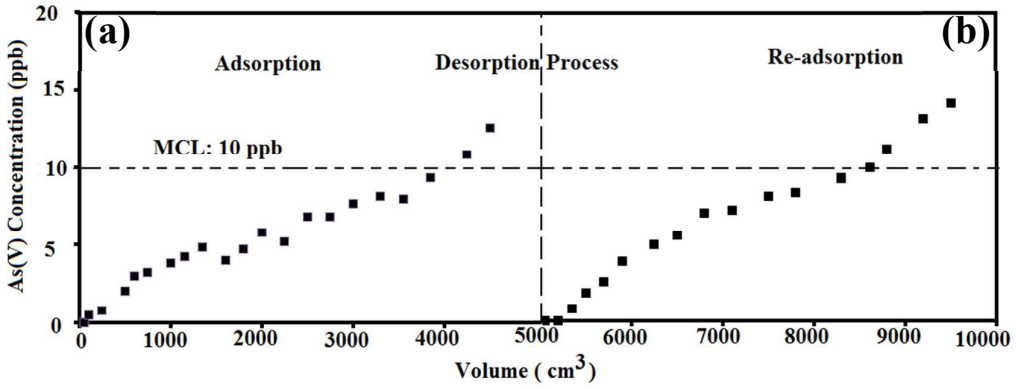

Fig. 12: Adsorptive removal of As(V) by cross-flow UF process from aqueous solution by the optimized PES/TNT-1.5 membrane: (a) virgin membrane and (b) regenerated membrane. Operating conditions: initial As(V) concentration = 97.5 μg/L, temperature =25°C , initial feed pH= 6-8, membrane effective area = 12.56 cm^2, membrane thickness = 250 μm and transmembrane pressure = 0.1 bar.

4. Conclusions

In this work, a new type of nanocomposite membrane with high adsorption capacity against As(V) and excellent water permeability (~1250 $L/m^2.h.bar$) was produced via non-solvent induced phase inversion process. The X-ray diffraction studies validated the existence of recognizable peak at 11.5° in the nanocomposite membrane indicating the successful impregnation of TNTs in the PES membrane matrix. The adsorption capacity of TNTs against As(V) was further verified by the

Fourier transform infrared spectroscopy analysis. With respect to surface roughness, it was found that the higher the quantity of TNTs in the membrane matrix, the higher the surface roughness. The increase in surface roughness can be associated to the nodular structure of TNTs incorporated in PES matrix. The scanning electron microscopy and energy-dispersive X-ray spectroscopy analysis confirmed the uniform dispersion and existence of TNTs without any significant nanotube mass agglomeration in the PES matrix. In terms of filtration performance, the combined effects of improved surface hydrophilicity, higher surface roughness and higher porosity mainly cause the considerable water flux enhancement in nanocomposite membranes. The results yielded from the batch As(V) adsorption tests showed that the PES/TNT nanocomposite membranes can be used for As(V) removal at broad pH range of 2-11. The best performing membrane (designated as PES/TNT-1.5) exhibited the highest As(V) adsorption capacity (124.9 mg/g), which is comparable to the most of the accessible adsorbents and other As removal methods well documented in other studies. The continuous UF experiment revealed that PES/TNT-1.5 demonstrated excellent capacity for effective As removal from water samples by generating high quality permeate with As concentrations below the acceptable maximum level of 10 μg/L. Additionally, the adsorption capacity of the nanocomposite membrane can be easily regenerated employing alkaline solution without any considerable loss of efficiency.

Acknowledgement

The authors would like to gratefully and sincerely thank for the research grant funded by Universiti Teknologi Malaysia (UTM) under flagship research project (Vot No. 01G46).

References

1. P.L. Smedley and D.G. Kinniburgh, *Appl. Geochem, 2002, **17,** 517-568.*

2. J.C. Ng, J. Wang and A. Shraim, *Chemosphere*, 2003, **52,** 1353–1359.

3. W. Tang, Y. Su, Q. Li, S. Gao and J. K. Shang, *J. Mater. Chem.A,* 2013, **1**, 830-836.

4. S. Atkinson, *Membr.Technol*, 2006, **2006**, 8-9.

5. R.Y. Ning, *Desalination*, 2002, **143**, 237-241.

6. S. Song, A. Lopez-Valdivieso, D. Hernandez-Campos, C. Peng, M. Monroy-Fernandez and I. Razo-Soto, *Water Res*, 2006, **40**, 364-372.

7. T. R. Harper and N. W. Kingham, *Water Environ. Res*, 1992, **64**, 200-203.

8. R. M. O. Mendoza, C.-C. Kan, S.-S. Chuang, S. M. B. Pingul-Ong, M. L. P. Dalida and M.-W. Wan, *J. Enviro. Sci. Health., Part A,* 2014, **49**, 545-554.

9. P. Mondal, A. T. K. Tran and B. Van der Bruggen, *Desalination*, 2014, **348**, 33-38.

10. B. Xi, X. Wang, W. Liu, X. Xia, D. Li, L. He, H. Wang, W. Sun, T. Yang and W. Tao, *Sep. Sci. Technol*, 2014, **49**, 2642-2649.

11. B. Chen, Z. Zhu, J. Ma, Y. Qiu and J. Chen, *J. Mater. Chem. A*, 2013, **1**, 11355-11367.

12. X. Yu, S. Tong, M. Ge, J. Zuo, C. Cao and W. Song, *J. Mater.Chem. A*, 2013, **1**, 959-965.

13. N. Mahanta and J. P. Chen, *J. Mater. Chem. A*, 2013, **1**, 8636-8644.

14. T.Dutta, C.Bhattacherjee and, *IN. J. ENG Res Technol, 2012,* ***9,*** 1-23.

15. F. Fu and Q. Wang, *J. Environ. Manag*, 2011, **92**, 407-418.

16. Z. Xu, Q. Li, S. Gao and J. K. Shang, *Water Res*, 2010, **44**, 5713-5721.

17. M. Hua, S. Zhang, B. Pan, W. Zhang, L. Lv and Q. Zhang, *J. Hazard. Mater*, 2012, **211**, 317-331.

18. K. Gupta and U. C. Ghosh, *J. Hazard. Mater*, 2009, **161**, 884-892.

19. S. R. Kanel, J.-M. Greneche and H. Choi, *Environ. Sci. Technol*, 2006, **40**, 2045-2050.

20. S. Bajpai and M. Chaudhuri, *J.Environ.Eng*, 1999, **125**, 782-784.

21. M. E. Pena, G. P. Korfiatis, M. Patel, L. Lippincott and X. Meng, *Water Res*, 2005, **39**, 2327-2337.

22. G.-S. Zhang, J.-H. Qu, H.-J. Liu, R.-P. Liu and G.-T. Li, *Environ. Sci. Technol*, 2007, **41**, 4613-4619.

23. M. Ranđelović, M. Purenović, A. Zarubica, J. Purenović, B. Matović and M. Momčilović, *J. Hazard. Mater*, 2012, **199**, 367-374.

24. J. Li, H. Chang, L. Ma, J. Hao and R. T. Yang, *Catalysis Today*, 2011, **175**, 147-156.

25. M. Jang, S.-H. Min, T.-H. Kim and J. K. Park, *Environ. sci. Technol*, 2006, **40**, 1636-1643.

26. Y. Du, H. Fan, L. Wang, J. Wang, J. Wu and H. Dai, *J. Mater. Chem. A*, 2013, **1**, 7729-7737.

27. S. Chatterjee and S. De, *Sep.Purif. Technol*, 2014, **125**, 223-238.

28. X. Guo, Y. Du, F. Chen, H.-S. Park and Y. Xie, *J. Colloid Interface Sci*, , 2007, **314**, 427-433.

29. B. Pan, B. Pan, W. Zhang, L. Lv, Q. Zhang and S. Zheng, *Chem. Engin. J*, 2009, **151**, 19-29.

30. R. Jamshidi Gohari, E. Halakoo, W.J. Lau, T. Matsuura, A.F. Ismail, *RSC Advances, 2014,* **4**, 17587–17596.

31. Y.-M. Zheng, S.-W. Zou, K. G. N. Nanayakkara, T. Matsuura and J. P. Chen, *J. Membr. Sci.*, 2011, **374**, 1-11.

32. R. Jamshidi Gohari, W. Lau, T. Matsuura and A. Ismail, *Sep. Purif. Technol*, 2013, **118**, 64-72.

33. H. Niu, J. Wang, Y. Shi, Y. Cai and F. Wei, *Microporous Mesoporous Mater*. , 2009, **122**, 28-35.

34. D. V. Bavykin, J. Friedrich and C. Walsh, *Adv. Mater.* , 2006, **18**, 2807-2824.

35. W. Liu, T. Wang, A. G. Borthwick, Y. Wang, X. Yin, X. Li and J. Ni, *Sci. Total Environ,* 2013, **456**, 171-180.

36. R. Jamshidi Gohari, W. Lau, T. Matsuura, E. Halakoo and A. Ismail, *Sep. Purif. Technol*, 2013, **120**, 59-68.

37 L. Xiong, C. Chen, Q. Chen and J. Ni, *J. Hazard. Mater*, 2011, **189**, 741-748.

38. P. Trivedi and L. Axe, *J. Colloid Interface Sci*, 1999, **218**, 554-563.

39. R. Jamshidi Gohari, E. Halakoo, N. Nazri, W. Lau, T. Matsuura and A. Ismail, *Desalination*, 2014, **335**, 87-95.

40. S. Singh and D. J. Keller, *Biophys. j*, 1991, **60**, 1401.

41. T. Wang, W. Liu, N. Xu and J. Ni, *J. Hazard. Mater*, 2013, **250**, 379-386.

42. M.-l. Luo, W. Tang, J.-q. Zhao and C.-s. Pu, *J. Mater. Process. Technol.* , 2006, **172**, 431-436.

43. S.-S. Liu, C.-K. Lee, H.-C. Chen, C.-C. Wang and L.-C. Juang, *Chem. Engin. J*, 2009, **147**, 188-193.

44. D. Mohan and C. U. Pittman Jr, *J.Hazard. Mater s*, 2007, **142**, 1-53.

45. G. Sheng, S. Yang, J. Sheng, D. Zhao and X. Wang, *Chem. Engin. J*, 2011, **168**, 178-182.

46. G. Zhang, J. Qu, H. Liu, R. Liu and R. Wu, *Water Res*, 2007, **41**, 1921-1928.

47. T.V. Nguyen, S. Vignes, *J. Hazard. Mater*, 2010,**182**, 723- 729.

48. Y.-M. Zheng, T.Matsuura, J.P. Chen, *J. Membr. Sci*, 2011, 374,1-11.

49. R. Chen, Z. Zhang, Z. Lei, N. Sugiura, *Desalination*, 2012, **286**, 56-62.

50. Z. He, S. Tian, P. Ning, *J. Rare Earth***,** 2012, **30**, 563-572.

51 C. Nieto-Delgado, J.R. Rangel-Mendez, *Water Res*, 2012, **46**, 2973-2982.

52. M. Mostafa, Y.-H. Chen, *J. Hazard. Mater*, 2011, **187**,89-95.

53 H. Akhter, L. Butler, S. Branz, F. Cartledge, *J. Hazard. Mater*, 1990, **24,** 145–155.

54 M. Taylor, R. Fuessle, Stabilization of Arsenic Wastes, HWRIC, Illinois, 1994.